Circular Array Retrodirective Action Using a Rotman Lens Beamformer

Circular Array Retrodirective Action Using a Rotman Lens Beamformer

Anil Chepala, Vincent Fusco, M. Ali Babar Abbasi
The Institute of Electronics, Communications and Information Technology (ECIT)
Queen's University Belfast, Belfast BT3 9DT, United Kingdom
achepala01@qub.ac.uk, v.fusco@ecit.qub.ac.uk, m.abbasi@qub.ac.uk

***Abstract*— We present the first use of a circular array for retrodirection covering full 360º. In particular, we discuss the attributes of the circular array when combined with Rotman beam forming. For reference the characteristics of the circular array when performing retrodirective action using local per element conjugation is also demonstrated. Simulated and measurement results at X-band are presented. The retrodirective circular array provides the advantage of 360° coverage when compared to other retrodirectors based on uniform linear arrays, as these typically allow only up to ±40° sector coverage.**

***Index Terms*—Circular array, retrodirective array, phase-conjugation.**

I. Introduction

A retrodirective array retransmits the received signal in the direction of the source without prior knowledge of source direction. Thus, they find application in communications [1], target tracking [2], and RCS enhancement [3]. In this paper, we show how a circular array equipped with a Rotman lens can be used for 360º azimuthal retrodirective beam steering. The design of circular arrays by modal analysis technique for beam forming and steering are discussed in [4 - 8]. The use of beamforming networks using the Rotman lens are described in [9], respectively. In [10] and [11] the use of a Rotman lens in a ULA based retrodirective array was discussed. We also show that by using a Rotman lens feeding a circular array we initiate retro directive application for full 360º coverage. We describe how the mechanism for retrodirective action using a Rotman lens is different from a Rotman lens fed retrodirective uniform linear array (ULA). In addition, for reference, we discuss the self-steering properties of the circular array when the signals arriving at the antenna elements in the circular array are individually and ideally phase conjugated.

Section II describes the principle of operation of the circular array along with a 12 element microstrip patch radiating element implementation. In section III, we discuss direct per-element phase conjugation and mode-pair interconnect methods for circular array retrodirection and present the measured results obtained for a Rotman lens fed circular array for retrodirective operation. Finally conclusions on the work are given.

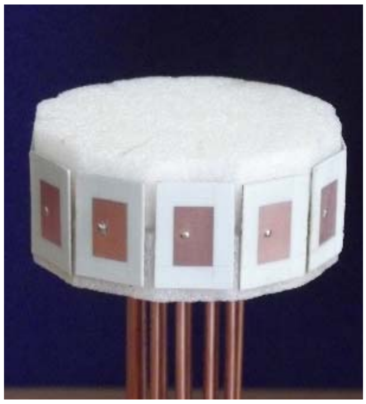

Fig. 1. Fabricated circular patch antenna array

II. Circular Array Design

A. General Circular Array Principle

The principle of operation of a multimode circular array is most easily seen by considering a continuous distribution of current, [7]. When this distribution is expressed as a Fourier series each term represents a current mode uniform in amplitude but having a linearly varying phase. The radiation pattern of each mode has the same form as the current mode itself, and these modes are themselves the Fourier components of the radiation pattern of the original distribution [4]. The horizontal far-field directional pattern '$F(\phi)$' of a continuous circular aperture is a periodic function with period 2π that can be expressed as a complex Fourier

$$F(\phi) = \sum_{m=-M}^{M} C_m e^{jm\phi} \tag{1}$$

where

$$C_m = \int_0^{2\pi} F(\phi) e^{-jm\phi} d\phi \tag{2}$$

When ϕ is the azimuth angle, M is the highest mode index and m is the mode number.

Here, if $B_K e^{j\beta_K}$ is the current applied to the K–th beam port of the beam forming network, the resultant current $A_J e^{j\psi_J}$ on the J–th radiating element connected to the array port is given by

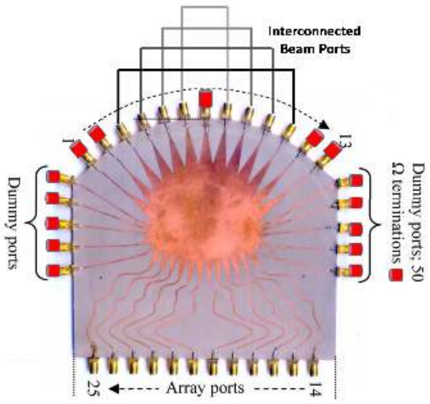

Fig. 2. Fabricated Rotman lens

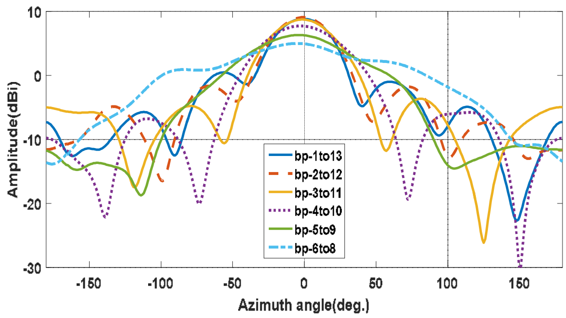

Fig. 3. Mode aligned beamforming circular array far-field directivity patterns.

$$A_J e^{j\psi_J} = \frac{B_K e^{j\beta_K} e^{jKJ\left(\frac{2\pi}{N}\right)}}{\sqrt{N}} \quad (3)$$

When many beam ports are simultaneously excited then the output current distribution is the summation over K for the N element array. Consequently, the far-field radiation pattern assuming the approximate pattern of dipole $A(\phi)$ as $0.5\times(1+\cos(\phi))$ is given by

$$E(\phi) = \sum_J \left[\sum_K B_K e^{j\beta_K} e^{jKJ(2\pi/N)} \right] \cdot A(\phi - \alpha_J) e^{j(\beta r)\cos(\phi - \alpha_J)} \quad (4)$$

When $\beta = 2\pi/\lambda$, λ is the wavelength of operation, and r is the radius of the array [4, 5], α_J is a general representation of element angular location in a circular array with N equally spaced elements at $\alpha_J = J2\pi/N$, when $J = 1,2, \ldots$ N. Referring to the circular array center, the relative phase of the J-th element in this case would be $(2\pi r/\lambda) \cos(\phi - \alpha_J)$.

B. Circular micro-strip patch antenna array

The radiating element for the demonstration array was chosen for ease of fabrication as a microstrip patch, operating at 9.3 GHz, and constructed on dielectric RO40003C (ϵ_r = 3.38 and *loss tangent* = 0.0027). The calculated dimensions for the above specifications are patch *width* = 10.14 mm, *length* = 7.52 mm, height h = 0.51 mm, and the substrate ϵ_{r-eff} = 3.13. The full–wave electromagnetic simulation based $|S_{11}|$ was below -10 dB at 9.5 GHz. A circular array with 12 elements (having an angular separation between neighboring elements = 30°) was designed with the above patch elements. The separation between the elements is 0.5λ and the diameter of the array is approximately 2λ, i.e. 60 mm at 9.3 GHz. The circular array was assembled on Styrofoam (see Fig. 1). The isolation between adjacent patches was < 25 dB.

A micro-strip based Rotman lens (RL) designed and fabricated in accordance with the method in [11] (see Fig. 2). The radiating elements are attached to the array ports while the interconnecting lines necessary for retro direction action are attached to complementary beam ports. The measured beam port $|S_{11}|$ are all below -10 dB and the nearest beam port-to-port isolation is better than 15 dB. Maximum lens insertion loss is 18 dB. When the modes of the CA are phase aligned [4], then summed, beam-forming occurs. From Fig. 3 we conclude that using ±4 modes with the RL and CA would yield reasonable results for beam-forming.

III. Retrodirective Circular Array

As explained earlier in the introduction a retrodirective array redirects incident signal back in the direction from which it came from. This can be made possible by conjugation of the phase received at each array element when the CA is illuminated with a plane wave whose polarization is matched to the patch array and which is applied at different angles of incidence (AOI). Here the antenna array elements are made to sample the signal incident upon them at the design frequency (i.e. 9.3 GHz). The induced signals at each of the array element circuit ports are conjugated, and are used to re-excite the array in transmit mode. The signals self-beam form to retrace their path back in the angle of arrival (AOA) from the signal source. The resulting simulated far-field radiation patterns under the above ideal phase conjugation voltages applied as excitation for the array in Fig.1 are shown in Fig. 4. These serve as a benchmark for comparing the RL method of retrodirection.

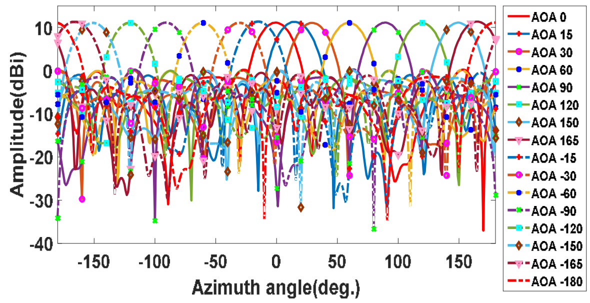

Fig. 4. Retrodirected far–field directivity patterns using direct conjugation.

The mode (beam port) terminals of an ideal RL, when paired in a mirror fashion, behave as phase conjugate of each other. The actual RL in Fig. 2 approximates this response. This property is exploited here for use in creating retrodirective action. This is achieved through mode pair RL beam port interconnection wherein mirror beam port pairs

TABLE I: Measured far-field results of retrodirective antenna array

Mode pair interconnection method –Angle of incidence /AOI (°)– Angle of return/AOR(°)																
AOI (°)	–165	–150	–120	–90	–60	–30	210	0	15	30	60	90	120	150	165	180
AOR(°)	–181	–155	–109	–84	–64	–26	–13	1	19	32	59	87	100	146	206	189
Gain(dBi)	5.8	7.7	6.2	8.5	7.6	8.0	7.6	8.3	7.0	7.6	8.1	7.7	6.2	7.3	5.0	3.7
3–dB BW(°)	57	43	81	41	49	47	51	45	57	51	45	51	78	47	103	91
SLL (dB)	–3.5	–6.1	–8.4	–8.4	–7.7	–7.6	–9.0	–8.9	–8.5	–6.7	–7.7	–7.8	–5.9	–4.8	–2.8	–1.4

are inter-connected using identical length transmission lines, Van Atta fashion, [10], see Fig. 2. Here individual conjugate mode pairs up to ±4 are strapped together at the RL beam ports, mode-0 (beamport 7 is short circuited) and the remaining beam ports are terminated to 50 Ω. With the RL beam ports interconnected in this way the measured far-field retrodirective monostatic patterns are shown in Fig. 5 and the main far-field pattern features summarized in table I.

When compared to the ideal retrodirection situation in Fig. 4, Fig. 5 shows retrodirection occurrence but there is a pattern distortion due to the operation of the RL at high angle of incidence, where internal reflections and port-to-port spillover occur [12]. This leads to reduced beam gain, and also increased side lobe level response of the retrodirected far-field pattern.

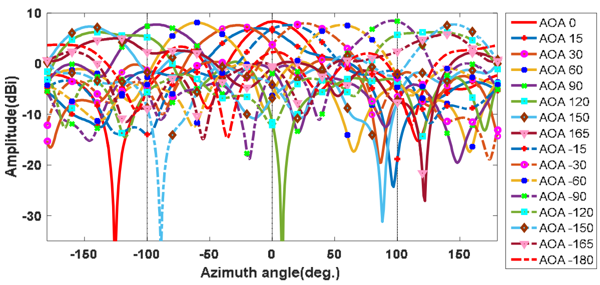

Fig. 5. Measured normalized retrodirected far–field patterns using mode pair interconnect.

It should be noted that retrodirection using a RL and ULA [11, 13], occurs using an operating principle that is different to the circular array. In the ULA case, the RL concentrates all of the incoming wavefront impinging on the ULA elements into a single beam port. Here it is reflected using an open- or a short- circuit, locally connected to that beam port. This then excites all of ULA array elements to a form the retrodirected signal. In a ULA the field of view over which an incoming wave front can be retrodirected is limited typically to ±45° due to mutual coupling variation between radiating with angle of arrival /departure. Whereas for a circular array mutual coupling remains constant with beam forming angle, [6].

IV. Conclusions

The operation of a twelve element circular array with a Rotman lens for retrodirection is presented. This shows the utility of using a Rothman lens in combination with a circular array for 360° sector coverage by retrodirection. The suggested technique should find application in radars and wireless communications.

Acknowledgment

The authors would like to acknowledge the PhD scholarship support given by the Queen's University Belfast and to the EPSRC under the grants EP/P000673/1, EP/NO20391/1. The authors would also like to thank Mr. Kieran Rainey for fabrication and testing of the circular patch array.

References

[1] K. M. K. H. Leong and T. Itoh, "Full-duplex retrodirective array using mutually-exclusive uplink and downlink modulation schemes," *2004 IEEE MTT-S International Microwave Symposium Digest (IEEE Cat. No.04CH37535)*, 2004, pp. 1695-1698 Vol.3.

[2] S. L. Karode and V. F. Fusco, "Multiple target tracking using retrodirective antenna arrays," *IEE National Conference on Antennas and Propagation*, York, UK, 1999, pp. 178-181.

[3] B. Y. Toh and V. F. Fusco, "Retrodirective array radar cross-section performance comparisons," *2000 High Frequency Postgraduate Student Colloquium (Cat. No.00TH8539)*, Dublin, 2000, pp. 65-70.

[4] B. Sheleg, "A matrix fed circular array for continuous scanning", *Proc. Of IEEE*, vol. 56, no. 11, Nov. 1968.

[5] V. Fusco, A. Chepala and M. A. B. Abbasi, "Target Location Using Dual Beam Directional Modulated Circular Array," in *IEEE Transactions on Antennas and Propagation*, 2018 (pre–print).

[6] T Rahim, "Directional pattern synthesis in circular arrays of directional antennas", PhD Dissertation, *University College London*, Aug. 1980.

[7] W. R. LePage, C. S. Roys, and S. Seely, "Radiation from circular current sheets", *Proc. IRE*, vol. 38.pp. 1069–1072, Sept. 1950.

[8] D. E. N. Davies, "Cylindrical Arrays with electronic beam scanning," *Proc. IEEE*, vol. 112, no. 3, Mar. 1965.

[9] E. O. Rausch and A. F. Peterson, "Rotman lens design issues," *2005 IEEE Antennas and Propagation Society International Symposium*, 2005, pp. 35-38 vol. 2B.

[10] L. Van Atta, "Electromagnetic reflector," U.S. Patent US2908002A, Oct.6, 1959.

[11] Y. Zhang, S. Christie, V. Fusco, R. Cahill and J. Zhang, "Retrodirective Rotman lens constraining factors," *2012 6th European Conference on Antennas and Propagation (EUCAP)*, Prague, 2012, pp. 2981-2984.

[12] M. Ali Babar Abbasi, H. Tataria, V.F. Fusco, M. Matthaiou, "On the Impact of Spillover Losses in 28 GHz Rotman Lens Arrays for 5G Applications", *IEEE MTT–S International Microwave Workshop Series on 5G Hardware and System Technologies,* Dublin, 2018.

[13] S. Christie et al., "Rotman Lens-Based Retrodirective Array," in *IEEE Transactions on Antennas and Propagation*, vol. 60, no. 3, pp. 1343-1351, March 2012.